THE EPOS SPECKLE FILTER: A COMPARISON WITH SOME WELL-KNOWN SPECKLE REDUCTION TECHNIQUES

Wilhelm Hagg, Manfred Sties
Institute of Photogrammetry and Remote Sensing
Karlsruhe University
Germany
Email: {hagg,sties}@ipf.bau-verm.uni-karlsruhe.de
Commission II, Working Group 4

KEY WORDS: Remote Sensing, Radar, SAR, Speckle, Multiplicative Noise, Edge Preserving Filters, Comparison

ABSTRACT

Any classification process using SAR images presupposes the reduction of multiplicative speckle noise, since the variations caused by speckle does not allow a distinction between neighboring classes within the feature space. This may be done by smoothing the images with digital filter algorithms, which removes the high frequent noise but also causes distortions at the high frequent image contents, i.e. sharp edges. Several adaptive filter algorithms have been developed, which aim at the preservation of edges and single scattering peaks, while homogeneous areas are smoothed as much as possible. This task is rendered more difficult by the multiplicative nature of the speckle noise: the signal variation depends on the signal itself. The recently developed EPOS speckle filter is compared with other well-known algorithms in this paper. In order to enable an objective comparison, the smoothing capability of all filters is adjusted to a similar value. To achieve a measurement for the quality, speckle is added synthetically to an image, so it is possible to calculate the RMS-error for each filtering method. Since the RMS differ according to the image contents, typical areas for several geometric objects are used to calculate the RMS. Also different signal to noise ratios are take into account in the comparison procedure to achieve an exhausting overview of the algorithm performance.

1 INTRODUCTION

The availability of optical remote sensing data for landuse applications is limited by the local weather conditions, especially by clouds. In addition illumination effects due to different sunsets aggravate the interpretation of optical datasets. Therefore "Synthetic Aperture Radar" (SAR) systems were developed which use their own, well defined, microwave illumination to penetrate clouds in the atmosphere. Another reason to develop SAR systems is the total different backscatter behavior of microwaves due to the long wavelength of microwaves relative to optical systems. There is a lot of operational SAR systems on satellite platforms available as the European ERS-1 and ERS-2, the Japanese JERS-1 and the Canadian RADARSAT. In addition several experimental systems were developed for a flight on board of a space shuttle. Recently the X-SAR/SIR-C mission resulted in the first spaceborn multi-frequency images of the earth surface; the instruments operate in the L- C- and X-Band. Also there exists a lot of airborne SAR-systems for experimental purposes.

While the SAR-systems and SAR-processors are in an operational state, the interpretation of SAR images is still under development due to several problems such as speckle noise and illumination effects in undulated terrain. SAR-processors are necessary to reconstruct the image from the synthetic aperture by coherently processing the returns from successive radar pulses along the flight path, and therefore they may be interpreted as the software component of the SAR instrument. Speckle noise is a system made consequence of the coherent radar illumination and appears as a granular pattern in the image. One of the most important feature of speckle noise is its multiplicative character which links the amount of noise to the signal intensity. The strong distortions of SAR images by speckle noise often prevent an useful application of SAR images in remote sensing. Thus, an effective reduction of speckle noise is one of the most important problems to solve for an operational SAR image interpretation.

Two categories of speckle reduction techniques are distinguishable; (1) the averaging of several looks of the same scene (multi-look processing), and (2) the smoothing of the image using digital image processing techniques. The multi-look processing is limited by the geometric resolution of the SAR instrument and the required resolution of the final image. For the geocoded standard ERS-1 products three independent looks are averaged to achieve a final resolution of about 25 meters. Both techniques use the fact, that averaging of several independent samples of a measurement reduces the variance of a signal. In the first case, several images are averaged, while in the second case values of neighboring pixels are averaged. The most simple way of smoothing images with digital image processing techniques is to apply a mean filter within a moving window around each image pixel. The result will be a smoothed image with reduced speckle variation, but edges and single point scatterers, as they appear in urban areas, are smoothed as well. Adaptive filter algorithms have been developed which aim at the preservation of edges and single scattering peaks, while homogeneous areas are smoothed as much as possible. For that purpose the filtering function has to be adapted to the local image contents to reduce the geometric distortions. It is obvious that the correction of a grey value, using the pixel values in the neighborhood, is efficient only in those cases where the neighboring pixels represents the same object on the ground.

Most filter algorithms for speckle filtering are not fully satisfactory for the purpose of SAR image classification, since the decrease of speckle caused variance is not sufficient for a distinction of neighboring classes within the feature space. Thus we developed a filter called EPOS (Edge Preserving Optimized Speckle-filter) which is published in (Hagg and Sties, 1994). The idea for the new algorithm was to adapt an area geometry to the image contents in such a kind, that the as-

sumption of a homogeneous area is given, which contains just variance caused by speckle. From that area we simply choose the mean as a new value for the filtered image. In order to determine homogeneity, the a priori knowledge of the coefficient of variation — that is the standard deviation related to the local mean — is necessary. This coefficient remains constant in homogeneous regions, where it is fully determined by the amount of speckle within the image. To find homogeneity even in heterogeneous regions and near edges, the averaging area is constructed from eight non-overlapping triangles around each pixel. This is done by successive elimination of triangles with the highest coefficient of variation, i.e. those containing an edge. If no homogeneous triangle was found, the observation window is reduced in its size and the procedure starts again. For single scattering peaks the area is reduced to one pixel and therefore no filtering is applied to those pixels. This enables a strong reduction of variation even in the neighborhood of edges and the preservation of edges as well as single scattering targets. The initial size of the observation window may be large, because it is reduced by the algorithm if necessary. Therefore the initial size of the window has less influence on the filtering result, if it is just large enough to enable an efficient reduction of the variation. This filtering algorithm will be compared with other filters in order to demonstrate the efficiency of different filters for individual tasks.

Most papers dealing with comparison of speckle filters use subjective criteria in order to compare the algorithms. Objective criteria are very hard to find, since the filters are adaptive to the signal and therefore measurements on a standard signals, as the impulse response of the filter, are not characteristic for the performance of the algorithm. In order to approximate an objective performance criterion we first analyze the requirements to speckle reduction. Since the distortions of edges and points within a filtered image increases with the decrease of noise, the amount of signal variation found in the filtered image is adjusted to a similar value for all algorithms. Most of the papers dealing with comparison of filters show the decrease of noise and the preservation of the image contents separately, thus an objective comparison is not provided. To achieve a measurement for the quality, speckle is added synthetically to an image, so it is possible to calculate the RMS-error for each filtering method. Since the RMS differ according to the image contents, typical areas for edges, lines and points are used to calculate the RMS. In addition different signal to noise ratios are used for the comparison to achieve an exhausting overview of the performance of the algorithms.

2 REQUIREMENTS OF SPECKLE FILTERING

As mentioned in the introduction, the rating of speckle filter performance using objective criteria is quite difficult, since the behavior of the adaptive filters used is extremely sensitive to the image contents. This results in a wide field of possible measurements which may be used as comparison criterion. Thus we first have to analyze the requirements to filter algorithms and derive comparison rules, in order to create rating criteria useful for practical applications.

In this paper we deal with landuse mapping as a frequently occuring remote sensing application. The main problem of the classification using SAR images is the spectral similarity of several classes. Meadows and water have similar signatures if the water surface is rough. Also the signatures of some loosely populated areas are similar to forest signatures. Conditioned by the high amount of speckle noise in SAR images, those classes may not be separated in the feature space which leads to an unacceptably high degree of misclassification. For this reason we found the main criterion for a speckle filter is to reduce the amount of speckle variance drastically. Using a mean filter with a 10 by 10 pixel averaging region will produce a higher accuracy as the classification of the original, speckled data. The loss of some geometric details is compensated by a much better distinction of class signatures, they appear more compact in the feature space. Therefore the radiometric image quality proofs to be the most important criterion for landuse mapping applications. On the other hand geometric distortions decrease the classification accuracy especially in heterogeneous regions containing relatively small fields of common semantic on the earth surface. Geometric objects may be grouped in areas, lines and points. Areas are typically build by classes as forest, water, meadow and agriculture, lines results from roads, railways and rivers. Points appear in urban areas as a result of double-bounds reflections and—depending on the resolution of the SAR—in other textured regions. Thus it is obvious that areas cover most of a SAR scene, followed by points and lines. According to the above geometric primitives, geometric distortions appear at edges between areas, lines and points within the image. Regarding just the edges of areas instead of the areas itself will also result in the fact, that edges cover much more of the image than lines and points. Of course this fact depends strongly on the area mapped, but it holds in large regions not just containing a local phenomenon like an urban area. Furthermore the distortions located at points may be compensated by the use of texture features in the classification process. Texture features are described in (Haralick, 1978), (Hagg et al., 1995) and many other publications.

Recapitulating this section, the radiometric enhancement of SAR images by reducing the speckle variance is the primary task to solve by speckle filter algorithms, while the problem of geometric distortion proofs to be secondary. The focus of interest regarding the geometric primitives is the distortion at edges between areas. Line and point features may decrease the classification accuracy less and therefore they may be rated more laxly in a comparison criterion. Depending on the application, other criteria may be suggestive, as it is for the extraction of linear features as roads from an image. For applications dealing with areas, the above mentioned criteria may hold generally.

3 FILTERING ALGORITHMS

Adaptive speckle filtering algorithms may be separated in two categories; (1) statistical algorithms, using the local statistic within the moving window to adapt the filter to the image contents and (2) geometric algorithms, which take into account the signal at different angular directions around each pixel. In opposition to one dimensional signals, where each sample value has just two neighbors, a pixel in an image is strong related to its environment. In addition to the distance relation of a one dimensional signal, the angle is a second relation for images. At a distance of one pixel, 8 different angels are distinguishable; in general for a n pixel distance $8n$ different pixels are related to the central pixel. This strong embedding of each pixel enables the extraction of information from different angles in order to optimize the filter adaption

to the local image contents.

An overview of the algorithms for various filters may be found in some review papers as (Lee et al., 1994) and (Shi and Fung, 1994) and will not be recapitulated in this paper. The original papers dealing with the algorithms used, along with the abbreviation used in this paper are as follows for the geometric algorithms:

EPOS Edge Preserving Optimized Speckle Filter (Hagg and Sties, 1994)

GEOM Geometric Filter (Crimmins, 1985)

R-LEE Refined Lee Filter (Lee, 1981)

and for the statistical algorithms:

FRO Frost Filter (Frost et al., 1982)

E-FRO Enhanced Frost Filter (Lopes et al., 1990b)

LEE Lee Filter (Lee, 1980)

E-LEE Enhanced Lee Filter (Lopes et al., 1990b)

KUAN Kuan Filter (Kuan et al., 1985)

G-MAP Gamma Map Filter (Lopes et al., 1990a)

4 COMPARISON CRITERIA

This section aims at the definition of criteria which are more objective than those used in other review papers. A unique criterion for the rating of speckle filters is not available, thus subjective criteria are used in most papers dealing with filter comparison. Since speckle filters are almost adaptive to the signal in order to preserve the image contents, measurements on standard signals may not be generalized to describe the performance of the filter. Non adaptive filters, which approximate a spectrum in the frequency domain as the mean filter, may be characterized by the impulse response which describes the behavior of the filter completely. Using filters adaptive to the signal statistic within a moving window requires the observation of different signal to noise ratios in order to determine the behavior of the filter. In addition, filters using a geometric approach, and therefore depending on the actual geometry of the image contents, require the observation of different geometric arrangements to characterize the performance of the algorithm. In order to compare the preservation of edges and points, a similar factor of speckle reduction for the filters observed must be supposed.

4.1 COMPARISON BASIS

There is a contradiction between the efficiency of image smoothing and the preservation of edges, lines and point objects within an image. Using a mean filter, the size of the filter matrix is bound to the smoothing capability; a large matrix results in a large number of samples for averaging. On the other hand, the blurring of edges within the image is extended to an area around the edge, which is limited by the filter matrix size, thus large matrices will result in more distortions of the image contents. Thus the radiometric and the geometric image quality show a contradictory behavior with regard to the matrix size. Adaptive filtering algorithms try to optimize both, the radiometric and geometric quality, but the contradiction is just understated not eliminated. In order to compare the filter performance it is obvious, that one of the quality criteria must be retained while the other one is explored. A method where the criteria are reckoned up proofs to be not practicable, since the relationship between the radiometric and the geometric quality depends on the adaptive algorithm used for filtering. Thus we try to adjust the radiometric quality of all methods compared, i.e. we fix the amount of reducing speckle variation. This radiometric quality may be calculated easily from a homogeneous region from the image. The geometric quality is then estimated in a more complicated procedure described below.

In Section 2 of this paper we regarded the radiometric quality of an image as the essential criterion for the purpose of image classification. For that reason we tried to reduce the image speckle by a large amount. Some implementations of the filters used are limited to a 11 × 11 matrix size. A mean filter with the corresponding matrix of size $N = 11$ and sample size $S = NN = 121$ reduces speckle variation by $R = \sigma/\sigma_0 = 1/\sqrt{S} = 1/11 = 0.0909$, where σ denotes the standard deviation of a homogeneous area within the filtered image, σ_0 that within the speckled image. The speckle reduction R of adaptive algorithms is quite less using the same matrix size, so we aim at a decrease of the standard deviation of 10 percent. Notice that the measurement of R is independent of the mean grey level since the multiplicative noise model also fits for the smoothed image. Therefore the factor within the standard deviation representing the mean cancels out in the nominator and the denominator. The measurement is done from some large homogeneous areas at several greylevels within a test image. Since the speckle reduction capability of most filters is adjustable only by the matrix size, it is hard to meet the above requirement. Another way to adjust the smoothing performance is to apply filters several times, as it is necessary for the GEOM filter. Other filter parameters are generally used to optimize the filter performance at edges and therefore they are not available to adjust the smoothing capability in homogeneous areas. A good compromise for the adjustment of the filter algorithms was found by the values shown in Table 1 which are used for all examinations. The total values of speckle reduction are shown in Section 5. The

FILTER	WINDOW	ITER	DAMP
EPOS	11	1	0.75
GEOM	11	4	–
R-LEE	9	2	–
FRO	11	1	10
E-FRO	11	1	10
LEE	11	1	–
E-LEE	11	1	5
KUAN	11	1	–
G-MAP	11	1	–

Table 1: Filter parameters

R-LEE filter algorithm reduces the variation less than other filters, since approximately one halve of the matrix elements is used to calculate a mean value. Applying two iterations at a 9 × 9 matrix size results in a speckle reduction similar to the other algorithms. Also with the GEOM filter 4 iterations was necessary to achieve approximately the same smoothing capability. The damping factor was adjusted by evaluating the rating criteria mentioned below for several values. Nevertheless unacceptably low speckle reduction values R are rejected from the list of parameters in order to obtain a close field of radiometric image quality.

4.2 SPECKLE NOISE

Speckle noise results from the overlay of phase-incoherent signals within each resolution cell. The incoherence is caused by different distances between the sensor and the earth surface. This overlay of signals may be calculated as a vector sum of complex signal vectors, where the phase of the vectors is randomly distributed. It can be shown that the signal created by the sum, which may be thought of as a random walk in a two-dimensional vector space, is exponentially distributed for an intensity image and has a Rayleigh distribution for the amplitude of the signal (Ulaby et al., 1982b). From this point of view it also clear, that the speckle noise is of a multiplicative nature, since the variations are generated by the signal itself using the random phase.

In practical applications the noise is often reduced by multi look processing which is done by averaging independent samples of several images. With an increasing number of samples averaged, the Rayleigh distribution of a signal approximates a Gaussian distribution. In the case of the ERS-1 GTC and GEC geocoded products three looks of an amplitude image are averaged and therefore we decided for simplicity to use a Gaussian distribution for the tests. From theory we know, that the coefficient of variation is

$$C = \frac{\sigma}{\mu} = \frac{0.523}{\sqrt{N}} = 0.302$$

for $N = 3$ looks, where σ denotes the standard deviation, μ the mean of the signal. In practice we got a value of approximately 0.17 for the coefficient of variation within the ERS-1 images. This discrepancy may be explained by the averaging done by the geocoding process and the resampling from a 12.5 to a 25 meter pixel size. Both procedures calculate a new pixel value from neighboring pixels within the original image, thus a kind of averaging is done which reduces the speckle caused variance of the image. To obtain realistic results for practical applications we use the value of $C = 0.17$ obtained from the SAR images also within the synthetic image.

Several filters need the noise level of the multiplicative speckle noise contained in the image. Some implementations use the equivalent number of looks (ENL) instead of the coefficient of variation. The ENL is defined by the noise of a one look intensity image as

$$ENL(I) = (1/C)^2$$

For the test image we obtain $ENL(I) = 34.6$ as input for the algorithms.

4.3 GEOMETRIC CRITERIA

On the basis of a similar smoothing capability using the filter parameters mentioned above, we may now establish criteria for the appraisal of the geometric quality of the filters. To establish a measurement for the quality, the use of synthetically generated data is helpful. This enables the calculation of the RMS-error between the filtered and the original, unspeckled image. To get results as objective as possible, several geometric arrangements have to be observed, since different filters may prefer some type of geometry. Thus we established a test image containing points of different size, lines of different orientation and thickness as well as areas limited by edges intersecting at different angles of 180, 135, 90 and 45 degrees. The areas are also arranged in different orientations. The test image is shown in Figure 1. The highlighted

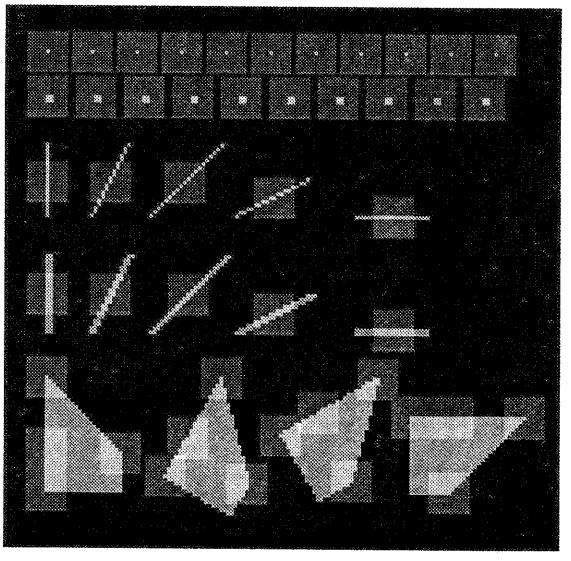

Figure 1: Test image with highlighted measurement areas

squares all over the image denote those areas, the RMS-error is calculated from. In order to determine just the geometric distortions and not the remaining variation all over the image, it is necessary to limit the measurement area to those pixels where the distortions occur. The RMS-error is calculated from each square by the formula

$$RMS = \sqrt{\frac{1}{N}\sum_{i=1}^{N}(\hat{x}_i - x_i)^2}$$

where N is the number of pixels within the square, x_i is the value of pixel i within the original image and $\hat{x}_i$ that from the filtered image. Since no substantial difference was found between different orientations and different angles between the area edges, a mean value for all points, lines and area features within the test image was calculated to reduce the amount of data and to get more reliable results.

Since adaptive filtering algorithms are sensitive also to the radiometry of an image, we duplicate the test image four times and use four different contrast values within the images, representing four different signal to noise ratios. The contrast values used are 100, 80, 60 and 40 greylevels difference between the dark and the light areas, equidistant from a level of 100. Calculating the sum of the 2σ distances of the Gaussian distributions results in a value of $d_s = 2\sigma_1 + 2\sigma_2 = 2(\mu_1 + \mu_2)C = 68$, where $C = 0.17$ denotes the coefficient of variation, σ and μ the standard deviation and mean of both distributions contained in an image. Thus the distributions intersect at their 2σ distance for a contrast value of 68. The first two contrast values don't have a significant overlay of the distributions, the last one results in an intersection near the 1σ distance.

4.4 OTHER CRITERIA

Another criterion which was valued is the retention of the mean value in homogeneous areas which is a need for several applications including image classification. Furthermore the computation time was measured in order to detect algorithms which are not applicable in practice due to the exhausting of computer resources. The results are presented in the following section.

TYPE	CONT	EPOS	GEOM	R-LEE	E-FRO	FRO	KUAN	LEE	E-LEE	G-MAP	MEAN
POINT	100	0.29	4.60	3.54	6.78	6.78	3.30	3.23	3.25	3.74	16.02
POINT	80	0.26	4.62	6.80	7.57	7.57	3.78	3.81	4.26	4.96	10.48
POINT	60	4.44	4.63	5.86	5.31	5.31	3.82	3.85	4.25	4.48	6.11
POINT	40	2.81	3.06	2.85	2.68	2.68	2.88	2.89	2.77	2.89	2.89
POINT	MEAN	1.95	4.23	4.76	5.59	5.59	3.45	3.45	3.63	4.02	8.88
LINE	100	2.49	13.70	10.58	10.40	10.40	11.44	11.46	12.80	12.95	150.00
LINE	80	2.61	14.03	12.23	12.52	12.52	12.48	12.55	12.98	14.99	96.47
LINE	60	21.75	14.81	17.48	20.11	20.11	12.81	12.84	13.01	17.21	54.87
LINE	40	23.87	14.72	22.84	15.96	15.96	11.46	11.35	12.66	16.80	25.01
LINE	MEAN	12.68	14.31	15.78	14.75	14.75	12.05	12.05	12.86	15.49	81.59
AREA	100	1.18	2.97	4.63	6.11	6.12	11.50	11.76	11.48	15.89	56.42
AREA	80	1.18	2.93	4.20	6.28	6.29	9.95	10.25	9.57	14.65	37.05
AREA	60	3.26	2.76	4.46	6.90	6.90	8.18	8.30	7.74	12.39	21.45
AREA	40	4.43	2.32	3.52	5.68	5.68	5.84	5.86	5.95	7.75	10.42
AREA	MEAN	2.51	2.74	4.20	6.24	6.25	8.87	9.04	8.68	12.67	31.34
MEAN	MEAN	5.71	7.10	8.25	8.86	8.86	8.12	8.18	8.39	10.73	40.60
RATED	MEAN	4.91	6.01	7.24	8.20	8.21	8.31	8.39	8.47	11.21	38.28

Table 2: RMS-error for different geometric primitives and contrast levels.

5 RESULTS

The basis of the comparison is the similar reduction of speckle variance in homogeneous areas for all filters. As mentioned in Section 4.1 this task is not easily solved, since a continuous parameter is not available to adjust the smoothing capability. The attempt to adjust all filters at a similar speckle reduction near $R = 0.1$ results in the values given in column two of Table 3. One should notice that especially the filters LEE, KUAN and G-MAP are adjusted to a quite less smoothing capability, thus geometric distortions may be less for those filters.

FILTER	REDUCT	M-ORIG	M-SPEC
MEAN	0.0963	-0.936	0.000
E-FRO	0.1065	-0.706	0.230
GEOM	0.1096	2.468	3.404
EPOS	0.1122	-0.874	0.062
FRO	0.1126	-0.458	0.478
E-LEE	0.1143	-0.438	0.498
R-LEE	0.1165	-1.460	-0.524
LEE	0.1309	-0.950	-0.014
KUAN	0.1328	-0.440	0.496
G-MAP	0.1363	-0.578	0.358

Table 3: Speckle reduction R and mean retention

The capability of mean retention is also shown in Table 3. Column 3 contains the difference of the mean within the filtered image and the original greylevel. Since the MEAN filter also shows a difference which is obviously caused by the noise, we subtract the value of the MEAN filter in column 4. The best values are obtained for the LEE and the EPOS filter, but most filters cover an uncritical range of 0.5 greylevels. Only the GEOM filter changes the mean in the homogeneous area by more than 3 greylevels, what is regarded as insufficient.

The most important criterion for the comparison, the distortions of the geometric primitives, is measured as RMS-error between the original, unspeckled and the filtered image. The results for various measurements are shown in Table 2. The first column denotes the type of the geometric primitive. The second column denote the radiometric contrast within the test image, representing different signal to noise ratios. For each geometric primitive one line shows the MEAN calculated from all contrast values. The last two lines show the mean of all geometric primitives, in the last line a rated value is shown where areas are weighted by $1/2$, points and lines by $1/4$ according to the significance of areas as considered in Section 2. The filter algorithms in Table 2 are sorted by the last line. The mean filter is also included in the table for a comparison.

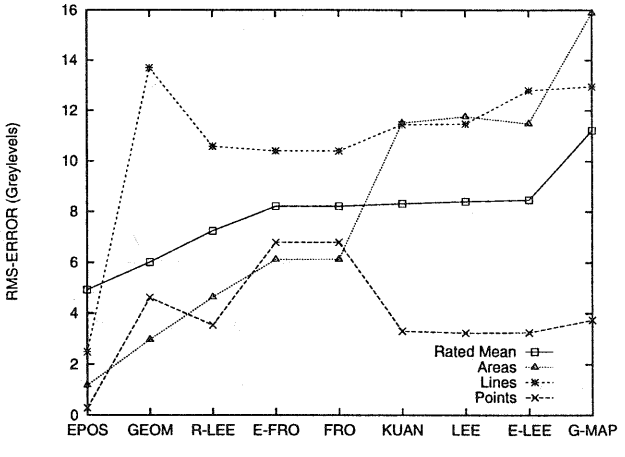

Figure 2: Distortions at geometric primitives (CONT = 100)

To illustrate the contents of the table, two diagrams are plotted from the lines of the table. Figure 2 shows the RMS-error of different filters for the geometric primitives at a contrast of 100 greylevels. It is significant that the EPOS filter perform much better than the other ones in all geometric disciplines for this high contrast. The RMS-error for different contrast values is shown in Figure 3 for areas. It is interesting that a reduction of the error with an increasing contrast is observed only with the EPOS filter. This reduction may be expected,

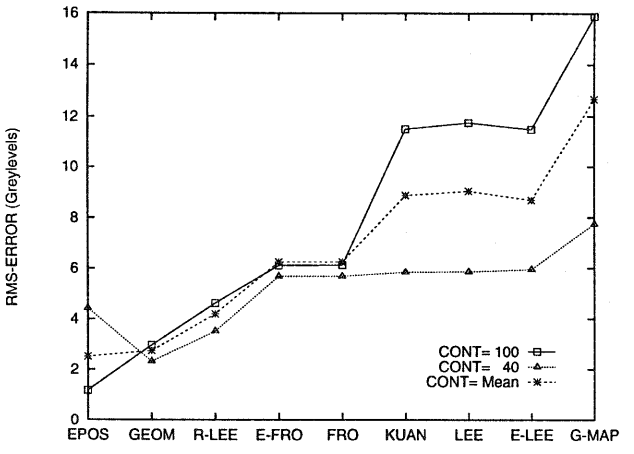

Figure 3: Distortions at different contrast values (Areas)

since an edge with a high contrast may be detected much better. For low contrast values the geometric filter seems to perform good for areas and lines, but even bad for points and according to the mean retention.

Finally the computation time needed on a sun sparc 20 for the test image was measured. Most filters are within a close field of $30 - 70$ seconds. Only R-LEE (112 sec.) and the GEOM filter (186 sec.) need more computation time since more than one iteration has to be performed. Since computer hardware performance increases very fast, we regard the computation time as a secondary criterion for a rating of the filters. The computation time of one ERS-1 scene at a 25 meter resolution is approximately 6 hours for the GEOM filter, what is practicable for most applications.

6 SUMMARY

A method has been presented to compare the performance of adaptive speckle filters in a more objective manner as it is done by other review papers so far. Therefore the smoothing capability of all filters in homogeneous areas was adjusted to a similar high level, as it is necessary to achieve a practicable radiometric image quality for several applications. On this basis the geometric distortions at different geometric primitives was measured by the RMS-error from a synthetic image. The method was applied to images at different signal levels with respect to the amount of speckle noise, thus we got an exhausting overview of the performance of various filter algorithms.

In general, algorithms which take into account geometric aspects, as the EPOS, GEOM and R-LEE filter, achieve the best overall performance, leaded by the EPOS filter. This is due to the evaluation of information, contained in two dimensional image signals by the strong embedding of each pixel in its environment, as mentioned in Section 3. Especially for signals at high contrast levels the EPOS filter outranges the other methods clearly, at low contrast levels some other filters perform somewhat better. Especially the GEOM filter seems to be preferable for the evaluation of areas and lines at low contrast levels, if the retention of the mean value is not necessary.

REFERENCES

Crimmins, T. (1985). Geometric filter for reducing speckle. In *SPIE, International Conference on Speckle*, volume 556, pages 213–222.

Frost, V., Stiles, J., Shanmugan, K., and Holtzman, J. (1982). A model for radar images and its application to adaptive digital filtering of multiplicative noise. *IEEE Transactions on Pattern Analysis and Machine Intelligence*, 4(2):157–166.

Hagg, W., Segl, K., and Sties, M. (1995). Classification of urban areas in multi-date ERS-1 images using structural features and a neural network. In *Proceedings IEEE International Geoscience and Remote Sensing Symposium*.

Hagg, W. and Sties, M. (1994). Efficient speckle filtering of SAR images. In *Proceedings IEEE International Geoscience and Remote Sensing Symposium*, pages 2140–2142.

Haralick, R. (1978). Statistical and structural approaches to texture. In *Proc. of the 4. Int. Conf. on Pattern Recognition*, page 45.

Kuan, D., Sawchuk, A., Strand, T., and Chavel, P. (1985). Adaptive noise smoothing filter for images with signal-dependent noise. *IEEE Transactions on Pattern Analysis and Machine Intelligence*, 7(2):165–177.

Lee, J. (1981). Refined filtering of image noise using local statistics. *Computer Vision, Graphics, and Image Processing*, 15:380–389.

Lee, J.-S. (1980). Digital image enhancement and noise filtering by use of local statistics. *IEEE Transactions on Pattern Analysis and Machine Intelligence*, PAM1-2(2):165–168.

Lee, J.-S., Jurkevich, I., Dewaele, P., Wambacq, P., and Oosterlinck, A. (1994). Speckle filtering of synthetic aperture radar images: A review. In *Remote Sensing Reviews*, volume 8, pages 313–340, USA. Harwood Academic Publishers.

Lopes, A., Nezry, E., Touzi, R., and Laur, H. (1990a). Maximum a posteriori filtering and first order texture models in sar images. In *Proceedings IEEE International Geoscience and Remote Sensing Symposium*, pages 2409–2412.

Lopes, A., Touzi, R., and Nezry, E. (1990b). Adaptive speckle filters and scene heterogeneity. *IEEE Transactions on Geoscience and Remote Sensing*, 28(6):992–1000.

Shi, Z. and Fung, K. B. (1994). A comparison of digital speckle filters. In *Proceedings IEEE International Geoscience and Remote Sensing Symposium*.

Ulaby, F., Moore, R., and Fung, A. (1982a). *Microwave Remote Sensing: Active and Passive*. Remote Sensing. Artech House, Inc., 685 Canton Street, Norwood, MA 02062.

Ulaby, F., Moore, R., and Fung, A. (1982b). *Microwave Remote Sensing: Active and Passive*, chapter 7, pages 464–483. Volume II of (Ulaby et al., 1982a).